Phase Diagram of the Orientationally Order-disorder Binary System 2,2-dimethyl-1,3-propanediol / 2,2-dimethyl-1,3-diaminopropane, $[(CH_3)_2C(CH_2OH)_2]_x$ $[(CH_3)_2C(CH_2NH_2)_2]_{1-x}$. A Thermodynamic, X-ray, and ^{1}H-NMR study

Roman Strauss[a], Sigmar Braun[b], Shi-qi Dou[a], Hartmut Fuess[a], and Alarich Weiss[c] (†)

[a] Fachbereich Materialwissenschaft, [b] Institut für organische Chemie, [c] Institut für Physikalische Chemie, Technische Hochschule Darmstadt, Petersenstrasse 20-21, D-64278 Darmstadt, Germany

Z. Naturforsch. **51 a,** 871–881 (1996); received February 23, 1996

The phase diagram of the binary system [2,2-dimethyl-1,3-propanediol]$_x$ **(1)** / [2,2-dimethyl-1,3-diaminopropane]$_{1-x}$ **(2)** was studied by X-ray diffraction and DTA/DSC, for **(2)** also by ^{1}H-NMR. The system is miscible over the whole concentration range $0 \leq x \leq 1$ in the liquid state and in the plastic solid state, phase I, just below the melting point. At lower temperatures the system is demixing, and at room temperature two plastic mixed crystals coexist. The plastic phases of **(1)**, **(2)**, and $(\mathbf{1})_x(\mathbf{2})_{1-x}$ crystallize face centered cubic, Fm3m, $Z = 4$, the lattice constants decreasing linearly with increasing x, and the lattice constants are: **(1)** $a_{(327K)} = 880.3$ pm , **(2)** $a_{(243K)} = 905.6$ pm. By single crystal X-ray diffraction the structure of the ordered phase II of **(1)** was refined at room temperature, monoclinic, $P2_1/n$, $Z = 4$, $a = 596.9$ pm, $b = 1090.2$ pm, $c = 1011.0$ pm, $\beta = 99.74°$. The results are in good agreement with the literature. The phase transition temperatures (in Kelvin) are $T_{I\rightarrow m} = 399.2$, $T_{m\rightarrow I} = 399.7$, $T_{II\rightarrow I} = 316.2$, $T_{I\rightarrow II} = 308.2$ for **(1)**; $T_{m\rightarrow I} = 300.2$, $T_{m\rightarrow I} = 301.7$, $T_{II\rightarrow I} = 228.7$, $T_{I\rightarrow II} = 194.2$ for **(2)**. Strong hysteresis is observed for the transition $T_{I\rightarrow II}$ in **(2)**. In the mixed systems $(\mathbf{1})_x(\mathbf{2})_{1-x}$, $0 < x < 1$, the disordered phases do not order even by quenching to liquid nitrogen temperature.

High resolution ^{1}H-NMR measurements are reported for phase I of **(2)** as a function of temperature. The "liquid" ^{1}H-NMR spectrum is present far below the thermodynamic phase transition temperature $T_{II\rightarrow I}$, overlapping the wide line unresolved powder spectrum of phase II.

Introduction

From thermodynamic studies [2 - 4] it is known that 2,2-dimethyl-1,3-propandiol, $(CH_3)_2C(CH_2OH)_2$**(1)**, is a two phase solid system with a high temperature orientationally disordered plastic phase I. For the low temperature phase II a monoclinic structure was reported [4 - 7], and the complete structure determination was recently published by Chandra et al. [1], who compared their results with the stucture data given by Zannetti [7]. Frank et al. report on DSC measurements as well as on X-ray powder diffraction of phase I, which is fcc [5]. The range of the plastic phase is rather wide, extending from $T_{II\rightarrow I} = 313.3$ - 316.2 K to the melting point $T_{I\rightarrow m} = 398.2$ - 399.2 K [3].

Several thermodynamic, spectroscopic (NMR), and crystallographic studies of polyalcohols are reported in the literature, including their binary systems because of their possible use for thermal energy storage materials of latent heat (see for example [8 - 29]).

In connection with our studies on orientationally disordered molecular solids, Cl_3CSO_2Cl [30], $Cl_3CSi(CH_3)_3$, $(CH_3)_3CSiCl_3$, $(CH_3)_3CSi(CH_3)_2Cl$ [31], and $(ClCH_2)_2C(CH_3)(COOH)$ [32] we extended our investigation to the phase diagram of 2,2-dimethyl-1,3-diaminopropane, $(CH_3)_2C(CH_2NH_2)_2$ **(2)**, which is isoelectronic with the diole **(1)**. This study revealed the existence of a plastic high temperature phase I for pure **(2)**. As a consequence, the question on the miscibility of the two title compounds in orientationally disordered and ordered phase arose, as the temperature ranges of phase I for both compounds are very different. We report here on thermodynamic, spectroscopic (NMR), and X-ray experiments to contribute to answers of these questions.

Reprint requests to Prof. Dr. H. Fuess.

0932-0784 / 96 / 0700-0871 $ 06.00 © – Verlag der Zeitschrift für Naturforschung, D-72072 Tübingen

Table 1. Thermodynamic data of 2,2-dimethyl-1,3-propanediol **(1)**, 2,2.dimethyl-1,3-propanediamine **(2)**, and the binary mixed system $[(CH_3)_2C(CH_2OH)2]_x[(CH_3)_2C(CH_2NH_2)_2]_{1-x}$. Temperatures are given in K, enthalpies ΔH in kJ/mol, entropies ΔS in J/(mol K), R = gas constant, * = this paper.

Binary mixed system $(\mathbf{1})_x(\mathbf{2})_{1-x}$

x	T_{on}	T_{end}	T_{m-1}	ΔH_m	ΔS_m	$\Delta S_m/R$
0.2	316.7	331.2	324.2	2.8	9.8	1.2
0.4	332.7	351.2	346.2	4.9	14.2	1.7
0.6	348.7	368.2	362.7	2.6	7.1	0.9
0.8	370.2	385.2	379.7	2.3	6.1	0.7

T_{I-II}	T_{II-I}	ΔH_{II-I}	ΔS_{II-I}	$\Delta S_{II-I}/R$	T_{m-I}	T_{I-m}	ΔH_{I-m}	$\Delta S_{I-m}/R$	Ref.
$(CH_3)_2C(CH_2OH)_2$ **(1)**									
308.2	316.2	13.7	43.2	5.2	399.7	399.2	4.7	1.4	*
—	315	13.8	43.8	5.3	—	403	4.6	1.4	[5]
—	313 - 316	13.6	43.1	5.2	—	398 - 399	4.7	1.4	[3]
—	313 - 316	13.6	43.4	5.2	—	398 - 399	4.7	1.4	[2]
$(CH_3)_2C(CH_2NH_2)_2$**(2)**									
194.2	228.7	14.7	50.9	6.1	300.2	301.7	1.7	0.7	*

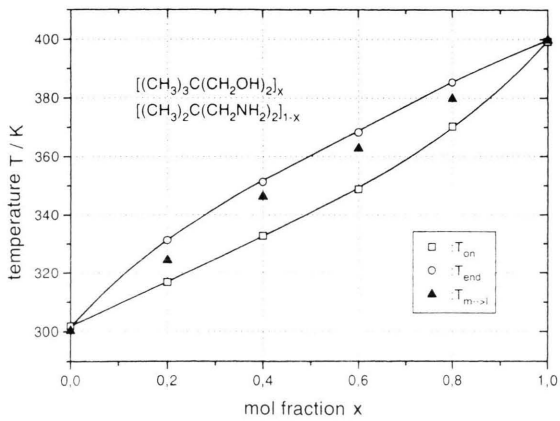

Fig. 1. Phase diagram for the binary system $(\mathbf{1})_x(\mathbf{2})_{1-x}$. T_{on}: start of the melting peak in the heating cycle; T_{end}: end of the melting peak in the heating cycle; T_{m-1}: solidification temperature of the melt in the cooling cycle.

1. Experimental

Commercial 2,2-dimethyl-1,3-propanediol **(1)** (Aldrich 99%) was purified by recrystallisation from toluene and sublimized in vacuum. The melting point of the compound purified in this way is 399.2 K, while [3] gives a melting point of 398.2 - 399.2 K. The purification of 2,2-dimethyl-1,3-diaminopropane **(2)** (Aldrich 99%) was achieved by fractional destillation twice in vacuo: It was handled under dry nitrogen atmosphere because of its highly hygroscopic behaviour. The observed melting point was 301.7 K.

The methods for the DTA/DSC experiments and the X-ray powder diffraction studies have been reported in [30 - 32]. For the single crystal X-ray work small crystals were selected and investigated on a Stoe-Stadi 4 diffractometer. The diffraction intensities were corrected for absorption and Lorentz-polarisation, the structure of **(1)** was solved by direct methods [33, 34].

The ^{1}H-NMR experiments were carried out on a Bruker ARX 300 high resolution spectrometer at 300.1333032 MHz with an offset frequency of 216 kHz. The samples were cooled (heated) with a temperature regulated nitrogen gas stream. The line widths of the resonance lines have been estimated graphically from the spectra.

Results and Discussion

Thermodynamic studies

In Fig. 1 the phase diagram of the system $(\mathbf{1})_x(\mathbf{2})_{1-x}$ as determined with DTA is shown. All samples including the pure components have been cooled down to about 160 K and then heated (1.5 K/min). In the cooling curves the transition plastic I → crystalline II was not detected for $0 < x < 1$ because of strong undercooling and formation of glassy plastic crystals in the mixed phases; so only the transition temperatures T_{m-I} are given in the figure. In the heating curves the melting peaks are broad up to 20 K between the onset temperature T_{on} and the end of the melting process T_{end}. Splitting of the peaks due to demixing within the plastic phase show the general transition from phases I to the melt. At lower temperature, first a diamine rich mixed crystal starts melting followed by a diol rich one. This demixing is confirmed by

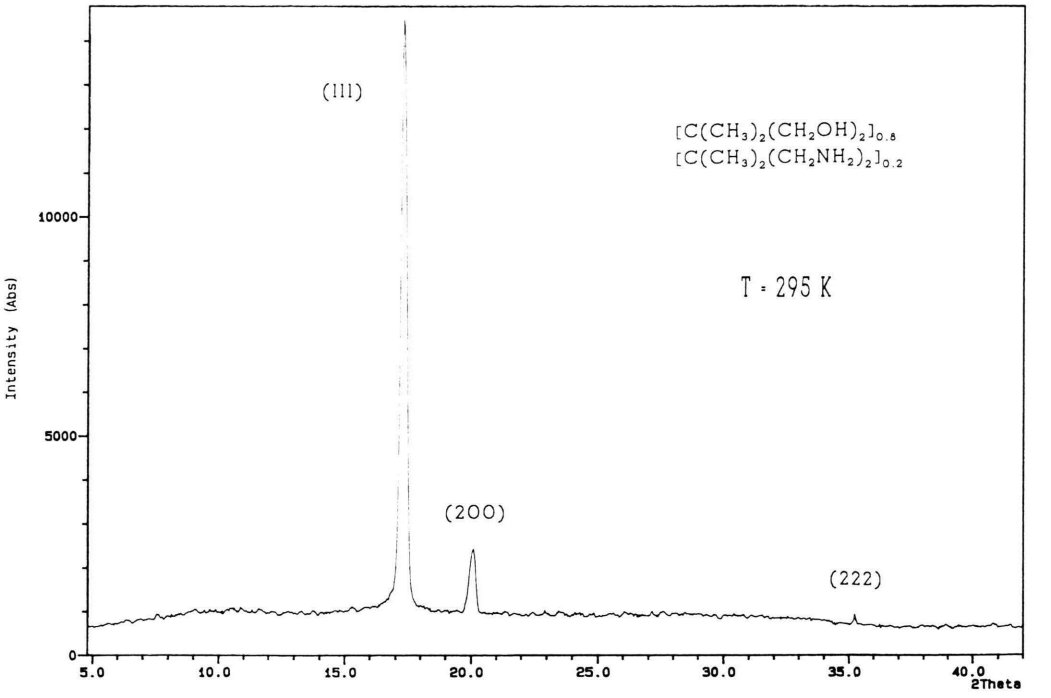

Fig. 2. X-ray powder diagram of plastic mixed crystal system $(\mathbf{1})_{0.8}(\mathbf{2})_{0.2}$. Radiation: $CuK_{\alpha 1}$, germanium monochromator (002), spectrometer: STOE STADIP, $T = 295$ K.

visual investigations which show definitely two optically isotropic phases for each mixture coexisting at room temperature.

In Table 1 we have summarized the thermodynamic data for the pure compounds, $x = 0$ and $x = 1$, of the system $(\mathbf{1})_x(\mathbf{2})_{1-x}$, including the data given in literature for **(1)** and some data for the mixed system.

X-ray diffraction

a) The Plastic Phases

In the system $(\mathbf{1})_x(\mathbf{2})_{1-x}$ an orientationally disordered phase I is observed for $0 \leq x \leq 1$ below the melting point. At room temperature ($T = 295$ K) X-ray powder diagrams have been taken for all mol fractions, and only one plastic phase per mixture could be identified via the three strongest reflexions (110), (200), and (222) of a cubic face centered structure. In Fig. 2. the powder diagram for $x = 0.8$ is shown as an example. This is understandable if we estimate roughly the mol fractions of the two inmiscible coexisting plastic crystals for a given general composition of the system from the phase diagram in Figure 1. Since these individual mol fractions never differ by more than $\pm$ 0.1 from the given composition, the expected two single powder spectra for each general composition are not resolved because of the too close lattice constants. The powder diffraction diagram with different scaling for pure **(2)** at $T = 243$ K is given in Figure 3. From the peak positions we derived for the fcc structure of **(2)** $a_{(243K)} = 905.6(7)$ pm and $a_{(327K)} = 880.3$ pm for compound **(1)**. Figure 4. displays the dependence of the lattice constants of the face centered cubic phases, Fm3m, $Z = 4$ for **(1)** and **(2)** as a function of temperature (the temperature ranges are different according to the difference in $T_{II \rightarrow I}$ for the two compounds). Figure 5. shows the lattice constant a for the binary system as a function of x at 295 K. The values for $x = 0$ and $x = 1$ are not measured directly but taken as extrapolations from the $a = f(T)$ measurements. For $a = f(x)$ we found $a/\text{pm} = 911.60 - 41.06x$. The linear thermal expansion coefficients $\alpha_{(T)} = a_{(T)}^{-1} \cdot (\mathrm{d}a/\mathrm{d}T)_p$ and the temperature dependence of

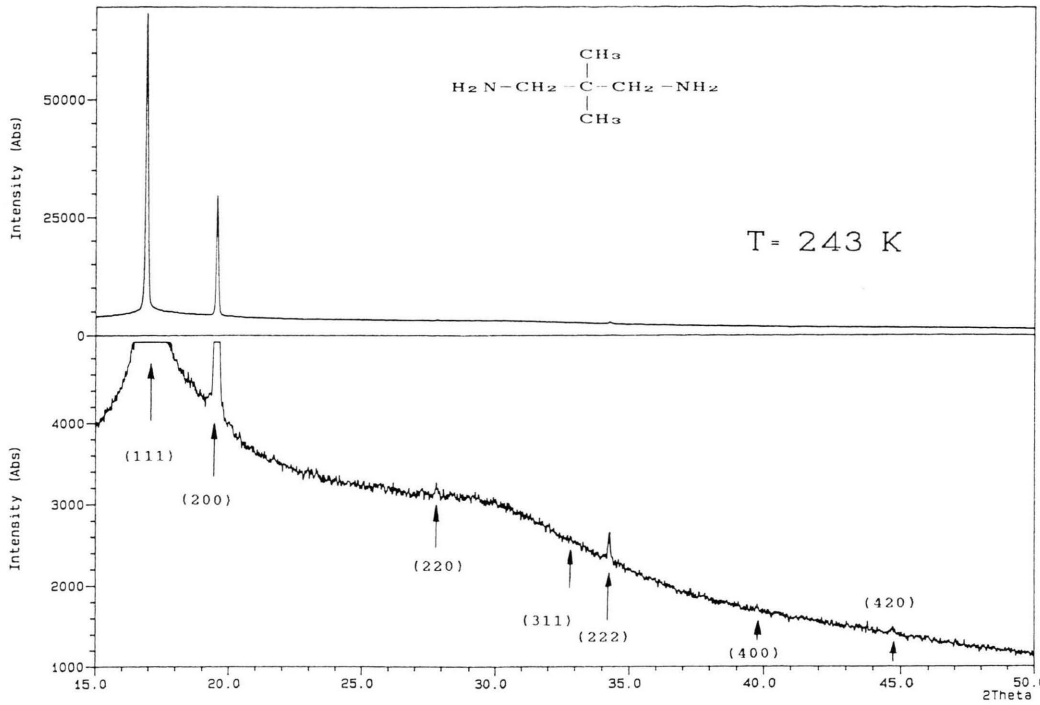

Fig. 3. X-ray powder diagram of the plastic phase I of pure **(2)**, $T = 243$ K.

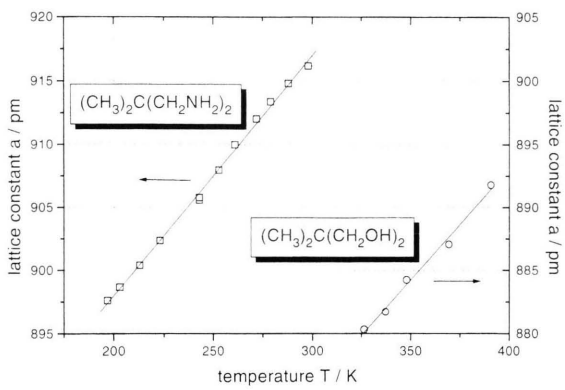

Fig. 4. Cubic lattice contants a of the plastic phases I of the pure compounds **(1)** and **(2)** as function of temperature.

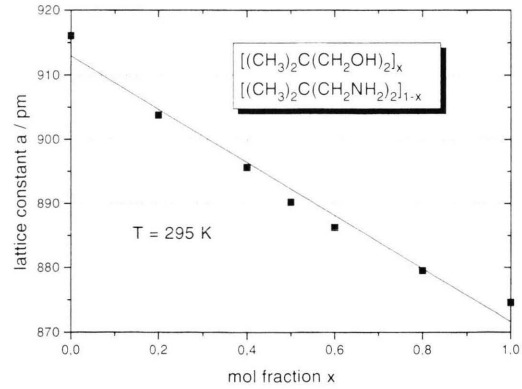

Fig. 5. Cubic lattice constants a of the plastic binary system $(\mathbf{1})_x(\mathbf{2})_{1-x}$ as function of mol fraction x at $T = 295$ K.

the lattice constant $a_{(T)} = a_0 + (\mathrm{d}a/\mathrm{d}T)_p \cdot T$ for **(1)** and **(2)** can be described as follows:

$(CH_3)_2C(CH_2OH)_2$ **(1)**: $\alpha_{(350K)} = 1.991 \cdot 10^{-4} \cdot K^{-1}$, $a/\mathrm{pm} = 822.61 + 0.1761 \cdot T/\mathrm{K}$;

$(CH_3)_2C(CH_2NH_2)_2$ **(2)**: $\alpha_{(273K)} = 2.085 \cdot 10^{-4} \cdot K^{-1}$, $a/\mathrm{pm} = 859.95 + 0.1901 \cdot T/\mathrm{K}$.

In spite of the different temperature ranges for the orientationally disordered phases I of the compounds

Table 2. Experimental conditions, crystal data, and structure refinement for the single crystal structure determination of the ordered phase II of 2,2-dimethyl-1,3-propanediol **(1)**, $(CH_3)_2C(CH_2OH)_2$, $C_5H_{12}O_2$, M = 104.17 g/mol. Diffractometer STOE-Stadi 4; wavelength: 71.069 pm (MoKα); monochromator: graphite (002); scan: $2\Theta/\omega$. The results are reported for the two settings $P2_1/n$ and $P2_1/c$. The values in brackets have been taken from the paper of Chandra et al. [1].

Setting		$P2_1/n$	$P2_1/c$
Crystal size / mm^3		4.00×0.15×0.10	
Temperature / K		302(2) [293(1)]	
Absorption coeff. μ / m^{-1}		48 [66]	
Θ-range for data collection		$2.77 \leq \Theta/° \leq 22.48$	
Index range		$-6 \leq h \leq 6$	$-6 \leq h \leq 6$
		$-11 \leq k \leq 0$	$0 \leq k \leq 11$
		$-10 \leq l \leq 10$	$-11 \leq l \leq 11$
Lattice constants / pm	a =	596.9(4) [597.9(1)]	596.9 (4)
	b =	1090.2(8) [1087.6(2)]	1090.2(8)
	c =	1011.0(8) [1009.9(2)]	1083.6(8)
	β =	99.74(3)° [99.78(1)]	113.14(3)°
$V\cdot10^{-6}$ / (pm^3)		648.4(8) [647.2(2)]	
rystal system		monoclinic	
Space group		C_{2h}^5-$P2_1/n$	C_{2h}^5-$P2_1/c$
Formula units Z		4	
ρ_{calc} / (Mg··m^{-3})		1.067 [1.069]	
F(0 0 0)		232	
Reflections collected		1789	
Symmetry independent		851 [887]	
data		851 [529] {R_{int} = 0.0236 [0.023]}	
Goodness of fit on F^2		1.041	
Restraints / parameters		0/85 [0/79]	
Final R (I > 2 σ (I))		R_1 = 0.0390 [0.043], wR_2 = 0.1075 [0.056]	
R indices (all data)		R_1 = 0.0584, wR_2 = 0.1270	
Extinction coefficient		0.13(2)	
Largest diff: (peak, hole) / (10^{-6} e / (pm^3))		0.098, –0.103	
Point positions		All atoms in 4*e*	

the thermal expansion coefficients are nearly identical and in the same order as typically for plastic crystals [30 - 32].

b) The Crystal Structure of the Ordered Phase II of 2,2-dimethyl-1,3-propanediol

Several previous studies of the crystal structure of phase II of **(1)**, also called neopentylglycol are reported. Zannetti [7] found from Weissenberg photographs a monoclinic unit cell with a = 598 pm, b = 1100 pm, c = 1081 pm, β = 112°24', ρ = 1.053 Mg/m^3. Nakano et al. [6] determined by single crystal Weissenberg technique the space group of the compound at room temperature as $P2_1/n$, a = 601 pm, b = 1090 pm, c = 1018 pm, β = 100.0°, Z = 4, but without any further information. By powder diffractometry Frank et al. [5] came to the same conclusions about the unit

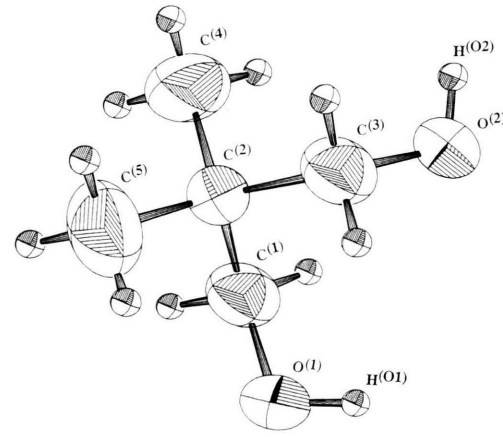

Fig. 6. The molecule of $(CH_3)_2C(CH_2OH)_2$ **(1)**, phase II, numbering of the atoms and thermal ellipsoids; the ellipsoids are at 50 % probability level (302 K), hydrogen atoms are drawn as spheres of abitrary size.

cell of phase II as [7]. They determined also the unit cell of the plastic phase I and found it to be fcc, a = 882 pm, Z = 4, ρ = 1.007 Mg/m^3 (T = 323 K).

From single crystal measurements the crystal structure of phase II was determined recently by Chandra et al. [1] in space group $P2_1/n$, and we have refined the crystal structure independently using a slightly different setting $P2_1/c$. For comparison with [1] we report here the structure of the ordered phase II of 2,2-dimethyl-1,3-propanediol also in their setting $P2_1/n$. The experimetal conditions for the crystal structure determination and crystallographic data are given in Table 2. The compound crystallizes in the space group $P2_1/c$, Z = 4, a = 596.9(4) pm, b = 1090.2(8) pm, c = 1083.6(8) pm, β = 113.14(3)°. Figure 6 presents a molecule with thermal ellipsoids for non hydrogen atoms and the numbering of the atoms throughout this paper. In Table 3 the coordinates of the atoms in the unit cell are listed as are the isotropic and anisotropic displacement factors. The coordinates of non hydrogen atoms are in both structure determinations within the limits of error identical. The thermal parameters given by Chandra et al. are slightly smaller. In Fig. 7 the unit cell is projected along the short axis [100] onto the *bc* plane. In Table 4 we report the intramolecular distances (bond distances) and angles, and in Table 5 the intermolecular distances, within the van der Waals contacts, and the hydrogen bond scheme are given. The differences in bond distances and angles agree within standard deviations except for d($O^{(1)}$-$H^{(O1)}$), d($O^{(2)}$-$H^{(O2)}$), and the angles $C^{(1)}$-$O^{(1)}$-$H^{(O1)}$,

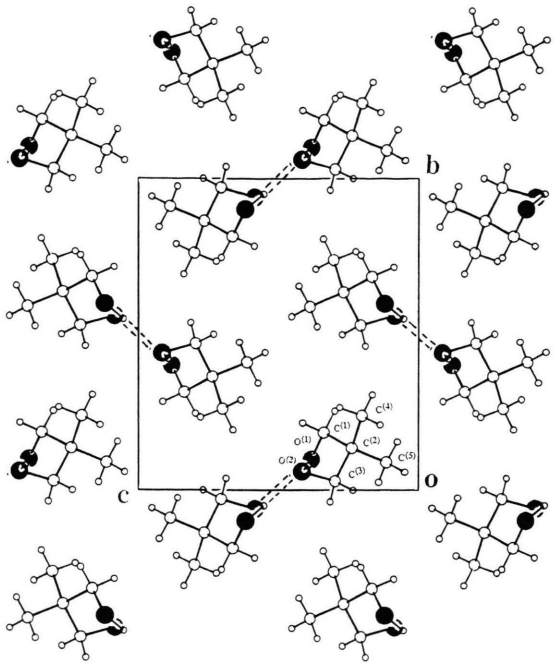

Fig. 7. Projection of the unit cell of **(1)**, phase II, along [100] onto the *bc* plane. The hydrogen bonds are marked by dashed lines.

$C^{(3)}$-$O^{(2)}$-$H^{(O2)}$, and as a consequence the hydrogen bonding.

In first approximation one could expect a highly symmetric molecule in the crystalline state characterized by the symmetry mm. The breakdown of the symmetry in the crystal field is due to an inequality of the two hydrogen bonds, the molecule forms in the ordered crystalline state. The deformations of the molecule are small. Bond distances *d*(C-C) are found between 151.1 pm and 152.3 pm, grouping around two centers, one for the $d(C^{(2)}\text{-}C^{(1,3)})$, 151.1 and 151.4 pm, respectively, and one for $d(C^{(2)}\text{-}C^{(4,5)})$, 152.1 and 152.3 pm. The difference in *d*(C-C) between the two groups may be significant, showing a shortening of a C-C bond due to a hydroxyl group attached to one of the carbons. The angles (C-C-C) are found between 107.8° and 111.5° without any systematic dependence on the OH group. The (C-C-O) angles are slightly widened (113.1° and 114.0°) compared with the angles (C-C-C).

The structure of the ordered phase of $(CH_3)_2C(CH_2OH)_2$ consist of pairs of tetrahedral molecules which are connected by hydrogen bonding to bimolecular chains. This arrangement of molecules

Table 3. Atomic coordinates ($\cdot 10^4$) and displacement parameters for $(CH_3)_2C(CH_2OH)_2$. The anisotropic displacement factor is of the form $T = \exp\{-2\pi^2 (h^2a^{*2}U_{11} + k^2b^{*2}U_{22} + l^2c^{*2}U_{33} + 2hka^*b^*U_{12} + 2hla^*c^*U_{13} + 2klb^*c^*U_{23})\}$. The isotropic displacment U_{eq} is defined as 1/3 of the trace of the orthogonalized tensor U_{ij}. The U_{eq} and U_{ij} are given in $(pm)^2$. The first set of data belongs to the setting $P2_1/n$ according to [1]; the second line gives the data for the setting $P2_1/n$ according to our refinement after transformation; the third line reports the results of our refinement, setting $P2_1/c$. The transformation of the coordinates is: $x(P2_1/c) = z(P2_1/n) - x(P2_1/n)$; $y(P2_1/c) = -y(P2_1/n)$; $z(P2_1/c) = z(P2_1/n)$. In [1] the displacement factors are given in $Å^2 \cdot 10^3$, so for comparison we have multiplied the data (including the error) by the factor 10.

Atom	*x* / *a*	*y* / *b*	*z* / *c*	U_{eq}
$C^{(1)}$	5556(5)	0286(3)	2962(3)	560(10)
	5553(4)	0290(2)	2957(2)	667(7)
	−2596(4)	−0290(2)	2957(2)	667(7)
$H^{(C1.1)}$	6463	8	2323	
	6457(4)	− 4(2)	2310(2)	800
	−4147(4)	4(2)	2310(2)	800
$H^{(C1.2)}$	4571	− 366	3147	
	4564(4)	− 374(2)	3136(2)	800
	−1428(4)	374(2)	3136(2)	800
$C^{(2)}$	4110(5)	1358(3)	2356(3)	500(10)
	4109(3)	1356(2)	2553(2)	569(7)
	−1756(4)	−1356(2)	2553(2)	569(7)
$C^{(3)}$	2746(6)	1860(3)	3368(3)	560(10)
	2750(4)	1851(2)	3368(2)	669(7)
	618(4)	−1851(2)	3368(2)	669(7)
$H^{(C3.1)}$	1825	2527	2959	
	1838(4)	2536(2)	2970(2)	803
	1132(4)	−2536(2)	2970(2)	803
$H^{(C3.2)}$	3783	2161(2)	4131(2)	
	3794(4)	2161(2)	4135(2)	803
	0342(4)	−2161(2)	4136(2)	803
$C^{(4)}$	5612(7)	2390(4)	1989(5)	900(10)
	5613(5)	2388(3)	1990(4)	1097(12)
	−3623(5)	−2388(3)	1990(4)	1097(12)
$H^{(C4.1)}$	6526	2121	1350	
	6497(5)	2097	1345	1316
	−5153(5)	−2097(3)	1345(4)	1316
$H^{(C4.2)}$	4639	3048	1608	
	4769(5)	3061(3)	1615(4)	1316
	−3064(5)	−3061(3)	1615(4)	1316
$H^{(C4.3)}$	6577	2675	2788	
	6612(5)	2658(3)	2783(4)	1316
	−3829(5)	−2658(3)	2783(4)	1316
$C^{(5)}$	2502(5)	0870(4)	1130(4)	940(20)
	2495(5)	0892(3)	1128(3)	1130(13)
	−1367(6)	−0892(3)	1128(3)	1129(12)
$H^{(C5.1)}$	1760	1595	0728	
	1549(6)	1554(3)	0736(3)	1356
	−0814(6)	−1554(3)	0736(3)	1356
$H^{(C5.2)}$	3333	0487	0508	
	3357(6)	0577(3)	0483(3)	1356
	−2874(6)	−0577(3)	0483(3)	1356
$H^{(C5.3)}$	1385	0307	1352	
	1559(6)	0251(3)	1393(3)	1356
	−0167(6)	−0251(3)	1393(3)	1356
$O^{(1.C1)}$	7010(4)	0598(3)	4165(2)	650(10)
	7017(3)	0598(2)	4159(2)	780(7)
	−2858(3)	−0598(2)	4159(2)	780(7)
$H^{(O1)}$	8271(77)	0679(35)	3904(37)	
	8252(62)	0778(27)	3953(29)	1008(106)
	−4299(59)	−0779(26)	3953(28)	1009(107)
$O^{(2.C3)}$	1312(4)	0980(3)	3822(2)	680(10)
	1309(3)	0983(2)	3817(2)	822(7)
	2508(3)	−0983(2)	3817(2)	822(7)
$H^{(O2)}$	2072(62)	0352(35)	4563(41)	
	2103(55)	0498(29)	4469(37)	1281(123)
	2364(61)	−0498(29)	4471(36)	1285(123)

Table 3 (cont).

Atom	U_{11}	U_{22}	U_{33}	U_{12}	U_{13}	U_{23}
$C^{(1)}$	540(10)	590(20)	550(20)	60(10)	80(10)	20(10)
	544(14)	706(15)	757(15)	78(11)	128(12)	6(12)
	572(14)	706(15)	756(15)	69(12)	298(12)	–6(12)
$C^{(2)}$	510(10)	600(20)	370(10)	40(10)	40(10)	110(10)
	473(11)	685(14)	552(12)	60(10)	97(10)	122(10)
	480(13)	686(14)	552(12)	–11(10)	214(10)	–122(10)
$C^{(3)}$	570(20)	530(20)	570(20)	50(10)	100(10)	50(10)
	547(14)	650(15)	812(16)	78(11)	119(12)	43(11)
	600(15)	650(15)	812(16)	50(12)	337(13)	–42(11)
$C^{(4)}$	800(20)	940(30)	1000(30)	50(20)	290(20)	540(20)
	810(20)	1226(24)	1317(26)	87(18)	357(19)	690(21)
	737(20)	1226(24)	1317(26)	–300(18)	392(19)	–691(21)
$C^{(5)}$	840(20)	1450(40)	470(20)	200(30)	–60(20)	–80(20)
	908(22)	1765(34)	636(16)	194(22)	–102(15)	–46(18)
	1088(25)	1764(34)	635(16)	206(23)	446(16)	46(18)
$O^{(1.C1)}$	470(10)	940(20)	510(10)	00(10)	20(10)	230(10)
	416(10)	1149(15)	752(11)	00(9)	34(8)	296(9)
	556(12)	1149(15)	752(11)	–163(10)	383(9)	–296(9)
$O^{(2.C3)}$	409(10)	950(20)	610(10)	10(10)	90(10)	270(10)
	447(10)	1177(15)	854(12)	–10(10)	143(8)	358(10)
	501(10)	1177(15)	853(12)	–207(10)	337(9)	–358(10)

Table 4. Intramolecular distances (bond lengths) *d*/pm and bond angles (in degree) in the unit cell of phase II of 2,2-dimethyl-1,3-propanediol. *d*(O-H) is found from difference fourier synthesis. The distances *d*(C-H) are fixed, $d(\text{C-H})_{\text{methyl}}$ = 96 pm, $d(\text{C-H})_{\text{hydroxymethyl}}$ = 97 pm. Also the angles C-C-H, H-C-H, and O-C-H have been fixed to 109.5(2)°, 109.5°, and 108.96(13)° or 108.76(13)° respectively. The data given in brackets are taken from [1].

Connection	*d* / pm	Connection	Angle / degree
$C^{(2)}$-$C^{(1)}$	151.4(3) [151.4(5)]	$C^{(4)}$-$C^{(2)}$-$C^{(5)}$	111.5(3) [112.0(3)]
$C^{(2)}$-$C^{(3)}$	151.1(3) [151.7(4)]	$C^{(1)}$-$C^{(2)}$-$C^{(5)}$	108.2(2) [107.8(3)]
$C^{(2)}$-$C^{(4)}$	152.3(4) [152.8(5)]	$C^{(3)}$-$C^{(2)}$-$C^{(5)}$	109.5(2) [110.2(3)]
$C^{(2)}$-$C^{(5)}$	152.1(4) [152.2(6)]	$C^{(1)}$-$C^{(2)}$-$C^{(3)}$	109.7(2) [109.9(2)]
$C^{(1)}$-$O^{(1)}$	141.1(3) [141.2(4)]	$C^{(1)}$-$C^{(2)}$-$C^{(4)}$	110.1(2) [109.6(3)]
$C^{(3)}$-$O^{(2)}$	140.6(3) [141.0(4)]	$C^{(3)}$-$C^{(2)}$-$C^{(4)}$	107.8(2) [107.3(3)]
$O^{(1)}$-$H^{(O1)}$	83(3) [106(4)]	$O^{(1)}$-$C^{(1)}$-$C^{(2)}$	113.1(2) [113.6(3)]
$O^{(2)}$-$H^{(O2)}$	91(3) [84(5)]	$O^{(2)}$-$C^{(3)}$-$C^{(2)}$	114.0(2) [112.9(3)]
		$C^{(1)}$-$O^{(1)}$-$H^{(O1)}$	107(2) [117(2)]
		$C^{(3)}$-$O^{(2)}$-$H^{(O3)}$	112(2) [102(2)]

in the lattice is quite different from that of pentaerythritol, $C(CH_2OH)_4$, which shows a layer structure [35]. The linear chains of $(CH_3)_2C(CH_2OH)_2$ form zig zag, alternating hydrogen bonds, and the chains are van der Waals bonded to the neighboring chains, as seen in Fig. 8, the projection of the unit cell along the twofold axis [010] onto *ac* plane. The hydrogen bond distances are rather short, 268 and 273 pm, partly responsible for the relatively high transition temperature $T_{\text{II}\rightarrow\text{I}}$, lying in the region of those in pentaerythritol.

^{1}H-NMR Study of Plastic $(CH_3)_2C(CH_2NH_2)_2$

The line width ΔB of the ^{1}H-NMR signals of 2,2-dimethyl-1,3-propanediamine, $(CH_3)_2C(CH_2NH_2)_2$,

Table 5. Intermolecular distances in phase II of (**1**) within the van der Waals distances (< 400 pm), minimum distance of neighboured central carbon atoms of molecules, and hydrogen bond scheme. Data of atoms that are marked (') are generated by given symmetry operations. The values in brackets have been taken from Chandra et al. [1].

Connection	*d* / pm	Connection	*d* / pm	Angle / degree
$C^{(4)}\cdots C^{(2')}$	390	$O^{(1)}\cdots O^{(2')}$	268(1)[272(1)]	
$C^{(5)}\cdots C^{(5')}$	394	$H^{(O1)}\cdots O^{(2')}$	187(4)[167(4)]	
$C^{(2)}\cdots C^{(2')}$	596	$O^{(2)}\cdots O^{(1')}$	273(1)[269(1)]	
$C^{(2)}\cdots C^{(2'')}$	580	$H^{(O2)}\cdots O^{(1')}$	184(4)[186(5)]	
$O^{(1)}$-H$\cdots O^{(2')}$				167(3)[173(2)]
$O^{(2)}$-H$\cdots O^{(1')}$				166(3)[164(2)]

$C^{(2')}$: $1-x, 1/2+y, 1/2-z$; $C^{(5')}$: $-x, -y, 1-z$;
$O^{(2')}$: $1+x, y, z$; $O^{(1')}$: $-x, -y, -z$.

and the chemical shift δ (towards TMS) of the methyl-, ethylene-, and aminoprotons was studied in the pure liquid phase, in solution with $CDCl_3$, and over a wide range in its plastic phase. In Fig. 9 the high resolution resonances in solution (T = 298 K) and the melt (T = 305 K) are shown. Both spectra look very similar. There is a small high field shift line broadening of the CH_2- and CH_3-protons in the melt compared with the dilute solution. However the frequency of the aminoprotons is shifted down field and also broadened. The chemical shift δ (in ppm/Hz) of the triplet spectrum in solution is 2.497/748.70 for CH_2-, 1.058/317.12 for NH_2-, and 0.832/249.57 for CH_3-protons. In the melt we found 2.400/720.35 for CH_2-, 1.274/382.42 for NH_2-, and 0.768/230.50 for CH_3-groups. The line width ΔB (in ppm/Hz) of the resonance signals at 305 K are 0.02/6.00 for CH_2-, 0.03/9.60 for NH_2-, and 0.023/6.90 for the CH_3-line. In addition the CH_2- and CH_3-lines are split to a triplet (in Fig. 9 because scaling not perceivable). The splitting is 0.01 ppm/3.1 Hz and 0.004 ppm/1.2 Hz for both triplets and due to spin coupling through the space by dipolar interaction in the melt. The signal of the aminoprotons is not split but broadened by exchange processes and quadrupole interactions. The down field shift of the NH_2-group in the melt can be explained in terms of a higher amount of hydrogen bonding between neighboring molecules in this phase in comparison to the dilute solution, where the molecules are separated from each other by molecules of the solvent.

In Figs. 10 - 12 the ^{1}H-NMR spectra of the solid plastic phase I of $(CH_3)_2C(CH_2NH_2)_2$ is shown in decreasing temperature steps of 10 K. It is remarkable that the triplet spectra are well resolved down to 223 K, showing the "liquid" like behaviour of

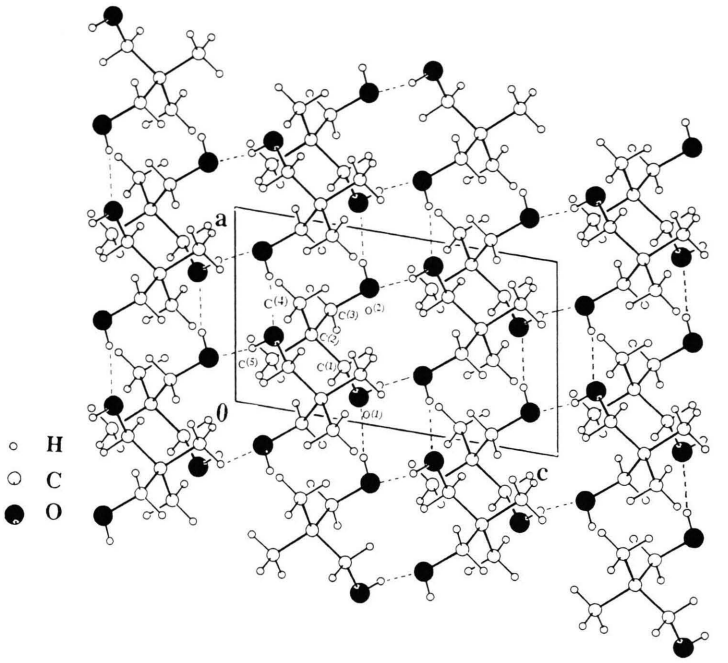

Fig. 8. Projection of the unit cell of the ordered phase II of $(CH_3)_2C(CH_2OH)_2$ along the axis [010] onto the *ac* plane. Hydrogen bonds are marked by dashed lines.

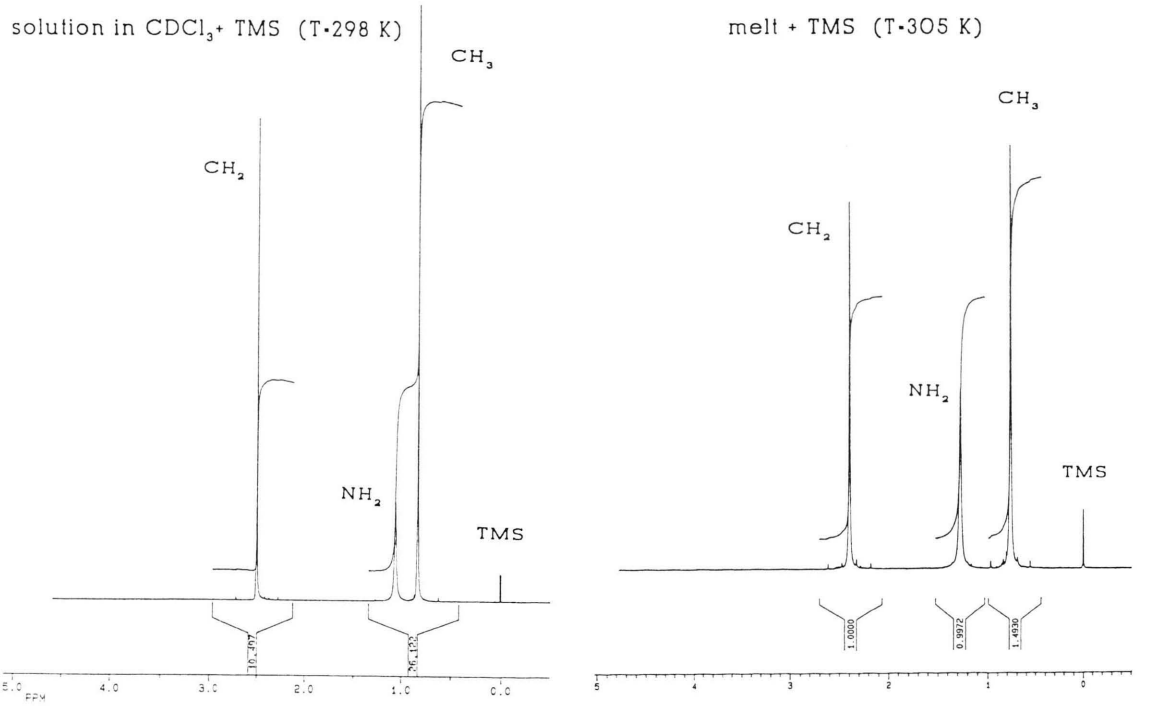

Fig. 9. ^{1}H-NMR spectra of $(CH_3)_2C(CH_2NH_2)_2$ **(2)** of solution in $CDCl_3$ + tetramethysilane (TMS) as standard at 298 K and of the molten pure compound + TMS at 305 K.

the molecules in this modification. The line width is increasing more and more with decreasing temperature because of higher dipole interactions between the molecules in the plastic phase. This is due to decreasing molecular motions and lattice contraction. The line width was derived by visual inspection.

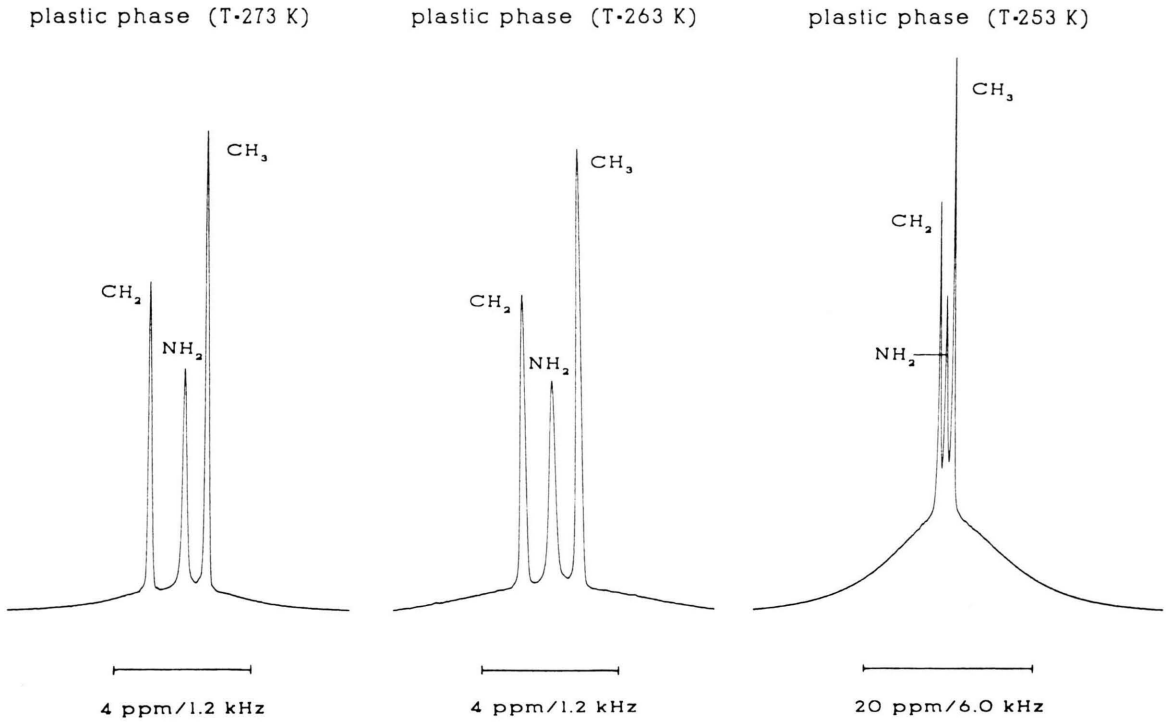

Fig. 10. ^{1}H-NMR spectrum of compound **(2)**, plastic phase I, at 273 K, 263 K, and 253 K.

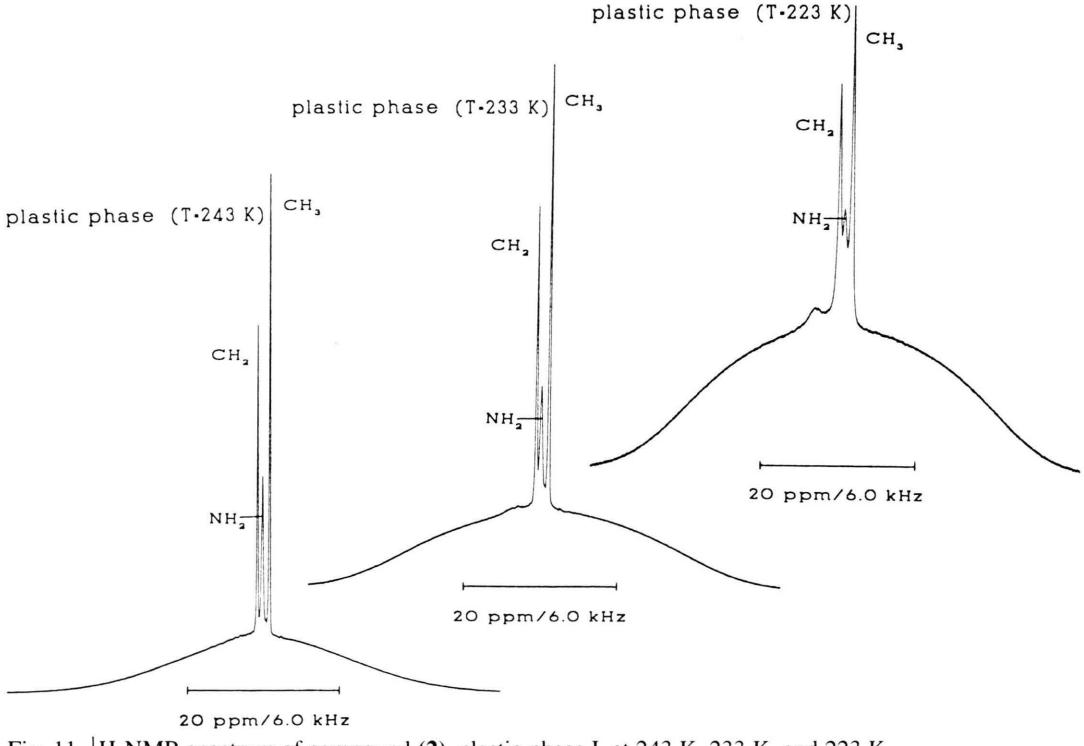

Fig. 11. ^{1}H-NMR spectrum of compound **(2)**, plastic phase I, at 243 K, 233 K, and 223 K.

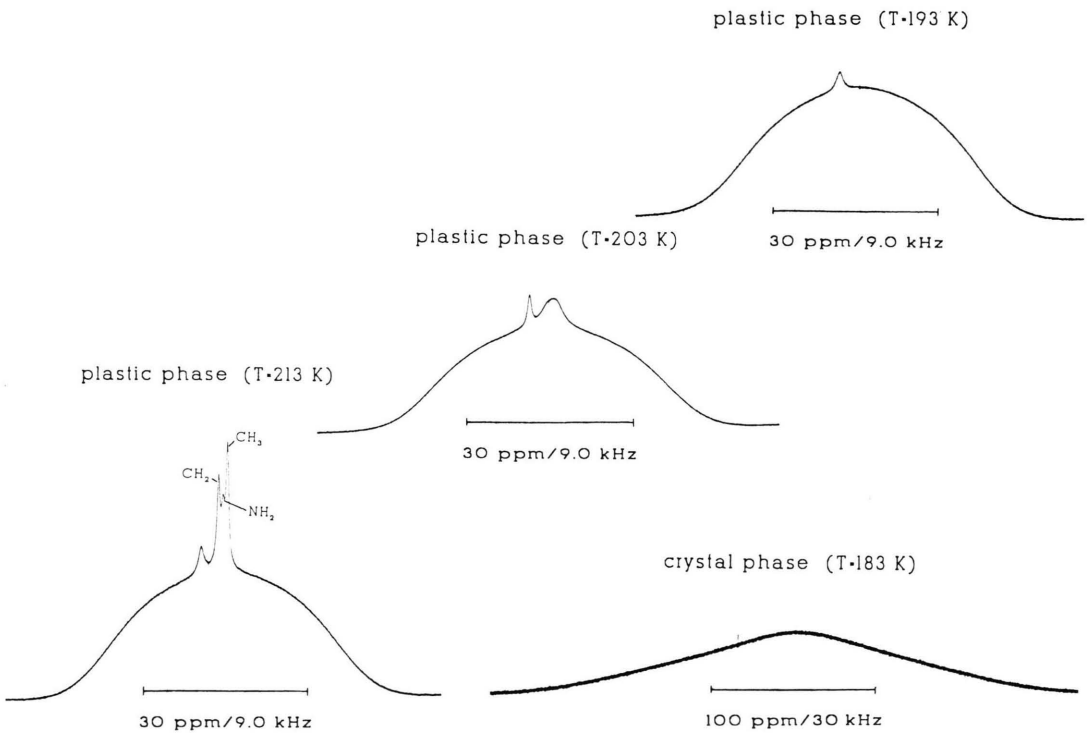

Fig. 12. ^{1}H-NMR spectrum of compound **(2)**, plastic phase I, at 213 K, 203 K, 193 K, and of the ordered crystalline phase II at 183 K.

Phase	T / K	Proton spezies CH_2 ΔB / Hz	δ / Hz	NH_2 ΔB / Hz	δ / Hz	CH_3 ΔB / Hz	δ / Hz	Total signal Triplet ΔB / Hz	Wide line ΔB / kHz
solution	298	—	749	—	317	—	250	—	—
melt	305	6	720	10	382	7	231	—	—
I	273	36	716	36	423	36	229	534	1.22
I	263	54	716	66	461	48	231	552	2.26
I	253	—	717	—	491	—	233	567	4.41
I	243	—	715	—	507	—	232	585	7.14
I	233	—	713	—	522	—	232	606	9.75
I	223	—	709	—	504	—	231	669	10.95
I	213	—	656	—	477	—	232	729	11.4
I	203	—	—	—	—	—	—	1235	11.6
I	193	—	—	—	—	—	—	—	11.8
II	183	—	—	—	—	—	—	—	42

Table 6. Line width ΔB of ^{1}H-NMR spectra of CH_2-, NH_2-, and CH_3-protons as well as of the total triplet in Hz and unresolved wide line in kHz as function of temperature. Also the chemical shift δ in Hz with respect to TMS for the individual proton spezies in melt m, solution ($CDCl_3$), and plastic phase I of $(CH_3)_2C(CH_2NH_2)_2$ is given.

Values for individual lines of the triplet were observed down to 253 K. At lower temperatures only the line width of the triplet as a whole is given in Table 6 together with the chemical shift towards TMS.

In addition the spectra show an increasing broad line band as background, on top of which the highly resolved triplet is observed. Below 233 K small domains of the crystalline phase II could give rise to such unresolved wide line resonances. At higher temperatures the origin of this background signal is not clear, but we think that the more or less isotropic reorientations of single molecules is replaced by reorientations of hydrogen bonded dimer or oligomer associations which show stronger dipole-dipole coupling and therefore a broad resonance line. Below 203 K the resolved triplet disappeared and only the

wide line spectrum is detectable. At 183 K the transition to the ordered crystalline phase II is complete and the line width approaches a magnitude similar to normal molecular crystals.

Acknowledgement

We are grateful to the "Deutsche Forschungsgemeinschaft" and the "Fonds der Chemie" for support of the work.

[1] D. Chandra, C. S. Day, and C. S. Barrett, Powder Diffraction **8**, 109 (1993).
[2] D. K. Benson, R. W. Burrows, and J. D. Webb, Sol. Energy Mater. **13**, 133 (1986).
[3] E. Murrill and L. W. Breed, Thermochim Acta **1**, 239 (1970).
[4] E. M. Schwarz, V. V. Grundstein, A. F. Ievins, A. A. Terauda, and A. A Vegnere, J. Therm. Anal. **5**, 665 (1973).
[5] H. P. Frank, K. Krzemicki u. H. Völlenkle, Chem. Ztg. **97**, 206 (1973).
[6] E. Nakano, K. Hirotsu, and A. Shimada, Bull. Chem. Soc. Jpn. **42**, 3367 (1969).
[7] R. Zannetti, Acta Cryst. **14**, 203 (1961).
[8] F. Wilmet, M. Ribet, P. Bernier, Y. Girault, and L. Elegant, Solid State Commun. **76**, 621 (1990).
[9] F. Wilmet, M. Ribet, P. Bernier, and L. Elegant, Solid State Commun. **83**, 961 (1992).
[10] M. Barrio, J. Font, J. Muntasell, J. Navarro, and J. L. Tamarit, Sol. Energy Mater. **18**, 109 (1988).
[11] M. Barrio, J. Font, D. O. López, J. Muntasell, J. L. I. Tamarit, N. C. Chanh, and Y. Haget, J. Chim. Paris **87**, 1835 (1990).
[12] M. Barrio, J. Font, D. O. López, J. Mutasell, and J. L. Tamarit, Calorim. Anal.Therm. **20-21**, 297 (1990).
[13] M. Barrio, J. Font, D. O. López, J. Muntasell, J. L. Tamarit, N. B. Chanh, and Y. Haget, J. Phys. Chem. Solids **52**, 665 (1991).
[14] D. Chandra and C. S. Barrett, Adv. *x*-Ray Anal. **29**, 305 (1986).
[15] D. Chandra, C. S. Barrett, and D. K. Benson, Adv. *x*-Ray Anal. **32**, 609 (1989).
[16] D. Chandra, R. A. Lynch, W. Ding, and J. J. Tomlinson, Adv. *x*-Ray Anal. **33**, 445 (1990).
[17] J. Font, J. Muntasell, J. Navarro, and J. L. Tamarit, Thermochim. Acta **118**, 287 (1987).
[18] J. Font, J. Mutasell, J. Navarro, and J. L. Tamarit, Sol. Energy Mater. **15**, 403 (1987).
[19] J. Font, J. Muntasell, J. Navarro, J. L. Tamarit, and J. Loveras, Sol. Energy Mater. **15**, 299 (1987).
[20] J. Font, D. O. Lopéz, J. Muntasell, and J. L. Tamarit, Mater. Res. Bull. **24**, 1251 (1989).
[21] P. Achard, M. Gabriel, D. Mayer, and L. Elegant, Calorim. Anal. Therm. **15**, 269 (1984).
[22] D. Mayer, P. Achard, and L. Elegant, Calorim. Anal. Therm. **16**, 481 (1985).
[23] D. Mayer, L. Elegant, and F. Wilmet, Calorim. Anal. Therm. **19**, P1.1 (1988).
[24] J. Mutasell, M. Barrio, J. Font, D. O. López, J. L. Tamarit, M. A. Cuevas Diarte, J. Guion, M. Teisseire, N. B. Chanh, and Y. Haget, J. Therm. Anal. **37**, 2395 (1991).
[25] M. Teisseire, N. B. Chanh, M. A. Cuevas-Diarte, J. Guion, Y. Haget, D. López, and J. Muntasell, Thermochim. Acta **181**, 1 (1991).
[26] F. Wilmet, N. Sbirrazzuoli, Y. Girault, and L. Elegant, Calorim. Anal. Therm. **20-21**, 251 (1990).
[27] D. Chandra, W. Ding, R. A. Lynch, and J. J. Tomlinson, J. Less. Common. Met. **168**, 159 (1991).
[28] M. Barrio, J. Font, D. O. López, J. Mutasell, J. L. Tamarit, P. Negrier, N. B. Chanh, and Y. Haget, J. Phys. Chem. Solids **54**, 171 (1993).
[29] M. Barrio, D. O. López, J. L. Tamarit, and Y. Haget, Mater. Res. Bull. **30**, 659 (1995).
[30] S. -qi. Dou, H. Fuess, H. Paulus, and Al. Weiss, Z. Naturforsch. **49a**, 174 (1994).
[31] S. Bräuninger, S.-qi Dou, H. Fuess, W. Schmahl, R. Strauss, and Al. Weiss, Ber. Bunsenges. Phys. Chem. **98**, 1069 (1994).
[32] R. Strauss, S.-qi Dou, H. Fuess, and Al. Weiss, Z. Naturforsch. **49a**, 1145 (1994).
[33] G. M. Sheldrick, SHEL*x*86. Program for the solution of crystal structures, University of Göttingen, Germany 1986.
[34] G. M. Sheldrick, SHEL*x*93. Program for crystal structure determination, University of Göttingen, Germany 1993.
[35] I. Nitta and T. Watanabõ, Bull. Chem. Soc. Japan **13**, 28 (1938).